Published in final edited form as:
*J Magn Reson Imaging*. 2014 February ; 39(2): 332–338. doi:10.1002/jmri.24151.

# 3D T2-weighted Spin Echo Imaging in the Breast

**Catherine J. Moran, PhD**[1], **Brian A. Hargreaves, PhD**[1], **Manojkumar Saranathan, PhD**[1], **Jafi A. Lipson, MD**[1], **Jennifer Kao, MD**[1], **Debra M. Ikeda, MD**[1], and **Bruce L. Daniel, MD**[1]
[1]Department of Radiology, Stanford University, Stanford, CA

## Abstract

**Purpose—**To evaluate the performance of 2D versus 3D T2-weighted spin echo imaging in the breast.

**Materials and Methods—**2D and 3D T2-weighted images were acquired in 25 patients as part of a clinically indicated breast MRI. Lesion-to-fibroglandular tissue signal ratio was measured in 16 identified lesions. Clarity of lesion morphology was assessed through a blinded review by three radiologists. Instances demonstrating the potential diagnostic contribution of 3D versus 2D T2-weighted imaging in the breast were noted through unblinded review by a fourth radiologist.

**Results—**Lesion-to-fibroglandular tissue signal ratio was well correlated between 2D and 3D T2-weighted images ($R^2 = 0.93$). Clarity of lesion morphology was significantly better with 3D T2-weighted imaging for all observers based on a McNemar test ($p \leq 0.02$, $p \leq 0.01$, $p \leq 0.03$). Instances indicating the potential diagnostic contribution of 3D T2-weighted imaging included improved depiction of signal intensity and improved alignment between DCE and T2-weighted findings.

**Conclusion—**In this pilot study, 3D T2-weighted imaging provided comparable contrast and improved depiction of lesion morphology in the breast in comparison to 2D T2-weighted imaging. Based on these results further investigation to determine diagnostic impact of 3D T2-weighted imaging in breast MRI is warranted.

### Keywords

T2-weighted; high-resolution; breast imaging; spin-echo; three-dimensional; extended echo train

## INTRODUCTION

T2-weighted imaging is a standard component of breast MRI exams. It is most prominently utilized for the identification of cysts but also can contribute to the characterization of lesions as benign or malignant (1–4). While the centerpiece of breast MRI remains T1-weighted dynamic contrast enhanced (DCE) imaging, both lesion signal intensity and morphology on T2-weighted images can also aid in differential diagnosis. The role of T2-weighted imaging in breast MRI has been investigated sporadically, with a few studies having demonstrated a potential contribution to improvement in specificity (1,3,5). Clinical evaluations of breast MRI also frequently incorporate acquisition of T2-weighted images (6,7). However, despite the well-established inclusion of T2-weighted imaging in breast MRI, the extent of its role remains vague. Recent studies continue to show the potential contribution of the technique to differential diagnosis (2) however, others point to the

Correspondence: Catherine J. Moran, PhD, Stanford University, Department of Radiology, Lucas Center for MR Imaging, Mail Code 5488, Route 8, Stanford, CA 94305-5488, fax (650) 723-5795, cjmoran@stanford.edu.

lingering questions about the significance of T2-weighted imaging as a part of routine breast MRI (8).

The challenge of determining a well-defined role for T2-weighted imaging in the breast is likely due, in part, to the technical limitations of efficient T2-weighted imaging, particularly in comparison to the highly efficient gradient-echo DCE acquisitions. Long repetition times are necessary with T2-weighted acquisitions to allow for T1 recovery, but echo train lengths are limited by the relatively short T2 times ($T2 \ll T1$). As a result, signal acquisition is only possible for a small percentage of the long repetition time, leading to excessive scan times for high-resolution imaging. In order to maintain reasonable scan times, conventional T2-weighted sequences use multi-slice 2D acquisitions with relatively low (~4mm) through-plane resolution often with slice gaps. The low through-plane resolution is also necessitated by the magnetization transfer effect on image contrast, which is exacerbated for very thin contiguous slices (9) in 2D multi-slice RARE (Rapid Acquisition with Relaxation Enhancement) (10) imaging. In addition slice profiles are distorted by gradient nonlinearities further confounding alignment between T2 and DCE findings. These inherent factors limit the full incorporation of T2-weighted imaging in breast MRI as the 2D multi-slice T2-weighted images are lower resolution and may suffer more distortion than their DCE counterparts.

Recently developed 3D T2-weighted sequences (11–14) have been designed to address the inherent challenges of fast T2-weighted imaging. Three-dimensional T2-weighted sequences utilize modified refocusing flip angle schedules, which preserve transverse magnetization, allowing for significantly longer echo trains (15). As a result, T2-weighted images with high resolution can be acquired in clinically feasible scan times. The ability to acquire T2-weighted images with a 3D excitation provides further benefits because magnetization transfer effects can be avoided and distortions due to gradient non-linearities can be corrected. While the modified flip angle schedules utilized in 3D T2-weighted imaging provide a means to overcome the inherent inefficiency of RARE imaging, they also introduce more complex stimulated echo pathways, the effect of which must be taken into account for their design and implementation in vivo.

The performance of 3D T2-weighted imaging has been investigated for a number of applications with varying results (16–20). In the ankle, the high-resolution 3D T2-weighted image volumes improved the depiction of diagnostic findings in any orientation (16). Uterine anomalies (19) and intraneural ganglion cysts (17) have been shown to be more clearly delineated using 3D T2-weighted acquisitions. In the knee, (20), the depiction of ligaments was equivalent between the 2D and 3D T2-weighted techniques but detection of meniscus tears was better with 2D FSE (Fast Spin Echo).

In this work, we investigate the performance of a 3D T2-weighted acquisition, 3D-FSE-Cube (14,21) in comparison to a conventional 2D T2-weighted acquisition (2D-FSE) in the breast. Both sequences were acquired in patients undergoing clinically indicated breast MRIs. The resultant images were analyzed for image contrast, depiction of lesion morphology, and potential for diagnostic impact. The goal of this work was to provide an initial evaluation of the consequences of replacing 2D T2-weighted imaging with 3D T2-weighted imaging in breast MRI, with analysis based on the aspects of T2-weighted images that have been shown to have the potential to contribute diagnostic information to breast MRI.

## MATERIALS AND METHODS

The 3D T2-weighted method utilized in this work is termed 3D-FSE-Cube (21) and is one of a class of sequences (11–14) that utilize specific refocusing flip angle schedules to maintain signal while extending echo trains. 3D-FSE-Cube utilizes an iterative process based on expected tissue parameters to determine the optimal refocusing flip angle schedule that quickly achieves a pseudo steady state with high signal (14). The signal is maintained for an extended period of time in comparison to the signal duration of conventional 2D T2-weighted sequences, thus allowing for more echoes per TR and a more efficient acquisition. In 3D T2-weighted imaging, stimulated echoes introduce T1 contamination to the signal and impact signal-to-noise ratio while the extended echo trains can cause tissue-dependent blurring. The effective image contrast of the sequence is dependent on the T1 and T2 of the tissues of interest and therefore may vary in vivo between applications.

In this study, 3D-FSE-Cube was assessed in comparison to 2D FSE, which is the sequence used to acquire T2-weighted images in routine breast MRI protocols at our institution. Twenty-five patients undergoing clinically indicated breast MRIs were scanned with both 2D FSE and 3D-FSE-Cube as part of their breast MRI. In 20 cases, patients were recruited consecutively. In the 5 other cases patients were recruited because of the known presence of a lesion based on biopsy or on previous imaging studies. All patients provided informed consent and all recruitment and consenting followed IRB institutional policies. In all cases, 2D FSE and 3D-FSE-Cube acquisitions were performed before the injection of contrast for the DCE acquisition.

Scans were performed on a GE Discovery MR 750 3T scanner (GE Healthcare, Waukesha, WI) with an 8-channel GE HD breast coil (GE Healthcare, Waukesha, WI). Imaging parameters for 2D FSE were as follows, and reflect the parameters utilized clinically at our institution: 32–38 cm FOV, 320 × 256 matrix, 4 mm slice thickness, 32–51 slices with no gaps, ETL 16, TR 3580 ms, scan time of 6 minutes, and TE of 98 ms. Imaging parameters for 3D-FSE-Cube were as follows: 30–33 cm FOV, 320 × 256 matrix, 2 mm slice thickness interpolated to slices every 1 mm, ETL 64, TR 2500 ms, scan time of 4 minutes, and TE 80 ms. For fat suppression 2D FSE utilized IDEAL (Iterative Decomposition of Fat and Water with Echo Asymmetry) (22,23). IDEAL is compatible with a number of different contrast mechanisms and is routinely used for fat suppression across a variety of clinical applications (22,24,25). The version of 3D-FSE-Cube utilized in this study employs spectrally-selective inversion for fat suppression. Both 2D FSE and 3D-FSE-Cube were acquired in the axial plane and utilized the auto-calibrating reconstruction for Cartesian (ARC) method (26,27) for parallel imaging. 2D FSE was accelerated by a factor of 3 in the phase encode (left/right) direction and 3D-FSE-Cube was accelerated by a factor of 2 in the phase encode (left/right) direction and a factor of 2 in the slice encode (superior/inferior) direction. Each case was analyzed for the presence of lesions by a radiologist with breast MRI expertise. Lesions were identified based on pathology or on contrast enhanced image assessment and/or stability from prior studies.

Image contrast was measured with a lesion-to-fibroglandular tissue signal ratio ($S_L/S_F$) for all identified lesion. Lesion signal intensity ($S_L$) was measured in an ROI placed in a central slice of each lesion and fibroglandular tissue signal intensity ($S_F$) was measured in an ROI placed in a region of fibrous tissue in the same breast as the lesion of interest. Correlation between $S_L/S_F$ of the two techniques was assessed with an ordinary least squares linear regression. Placement of ROIs was the same for each pair of images. Since T2-weighted signal intensity can vary across the breast, effort was made to place ROIs in regions of fibroglandular tissue with the most homogeneous signal. To evaluate the variability in the signal measurement within each ROI, the average percent error (STD/mean) was calculated

for each category of signal: 2D-FSE fibroglandular tissue signal, 2D FSE lesion signal, 3D-FSE-Cube fibroglandular tissue signal, and 3D-FSE-Cube lesion signal.

Three radiologists with breast imaging expertise performed a blinded paired review of identified lesions to assess the depiction of lesion morphology. Lesions demonstrating high signal intensity on the T2-weighted images were included in this review. Only lesions with high T2 signal were included because they could be localized without referencing the DCE images. This assured that the impression of lesion morphology for this comparison was based solely on the T2-weighted images. For each case, a single 2D FSE and a single 3D-FSE-Cube image were shown side by side cropped and magnified around the lesion with an arrow to indicate the lesion of interest (Figure 1). The order of the images within each pair was randomized and slice location was matched between the two methods. For each pair of images, the radiologist was asked to indicate in which image lesion morphology was depicted more clearly, or if the depiction of lesion morphology was equivalent between the two. A McNemar test was utilized to assess the results of this blinded paired comparison with statistical significance set at $p < 0.05$.

To assess the potential effect on diagnostic information of 3D-FSE-Cube versus 2D FSE, a fourth radiologist with breast MRI expertise performed an unblinded review of the 2D FSE and 3D-FSE-Cube images in context of the full breast MRI exam. All cases were included in this review. The radiologist first evaluated the DCE images with only the 2D FSE images included and then reviews the cases again 3D-FSE-Cube images incorporated. Instances where the 3D-FSE-Cube images contributed diagnostic information were noted. Both the 2D FSE and 3D-FSE-Cube images were reviewed in the axial orientation in which they were acquired as well as in reformatted sagittal and coronal orientations.

## RESULTS

For the 25 cases included in the study, the clinical indications were high-risk screening (13), preoperative staging (4), response to treatment (5) and diagnostic (3). A total of 17 lesions were identified in 11 patients, 10 based on pathology and 7 based on image assessment and/or stability from prior studies. Seven lesions were malignant (all invasive ductal carcinoma) and 10 were benign (5 fibroadenomas, 3 cysts, 1 cyst/hematoma, 1 papilloma). $S_L/S_F$ was well correlated between 2D FSE and 3D-FSE-Cube (Figure 2). Ordinary least squares linear regression demonstrated this agreement with a correlation coefficient of $R^2 = 0.93$. One IDC (invasive ductal carcinoma) was excluded from $S_L/S_F$ analysis because the breast was mostly fatty so there was insufficient fibroglandular tissue in which to measure signal. With 2D FSE, $S_L/S_F$ ranged from $0.57 \pm 0.11$ to $1.30 \pm 0.05$ with a mean value of $1.01 \pm 0.21$ for malignant lesions and from $0.84 \pm 0.14$ to $4.29 \pm 0.08$ with a mean value of $2.05 \pm 0.65$ for benign lesions. With 3D-FSE-Cube, $S_L/S_F$ ranged from $0.48 \pm 0.29$ to $1.39 \pm 0.21$ with a mean value of $0.99 \pm 0.25$ for malignant lesions and from $1.30 \pm 0.21$ to $4.14 \pm 0.16$ with a mean value of $2.16 \pm 0.62$ for benign lesions. The average percent error (STD/Mean) for each of the four categories of measurements (2D FSE fibroglandular tissue: 0.19, 2D FSE lesion: 0.26, 3D-FSE-Cube fibroglandular tissue: 0.20, 3D-FSE-Cube lesion: 0.29) indicated that variability in the measurement of signal intensity was comparable for the two techniques.

The comparable contrast between 2D FSE and 3D-FSE-Cube is demonstrated in a case that included both an IDC and an enhancing fibroadenoma (Figure 3). In this case, both the IDC and the fibroadenoma demonstrate increased signal due to contrast uptake in the DCE images. In the corresponding 2D FSE and 3D-FSE-Cube images, the IDC is isointense with respect to the surrounding fibroglandular tissue while the fibroadenoma is hyperintense with respect to the same tissue.

Ten benign lesions demonstrated high T2 signal and were included in the blinded paired review to assess depiction of lesion morphology. The 10 benign lesions were from 5 patients. 3D-FSE-Cube provided improved depiction of lesion morphology in comparison to 2D FSE for lesions with high T2 signal. The improvement was significant for all three observers ($p \leq 0.02$, $p \leq 0.01$, $p \leq 0.03$) based on a McNemar test. Clarity of lesion morphology in the 3D-FSE-Cube images was rated to be either equivalent to or better than that in the 2D FSE images by all three radiologists for all lesions (Figure 4). The improved depiction of lesion morphology is demonstrated in a cyst/hematoma (Figure 1) in which an increased gradation of signal levels is evident in the 3D-FSE-Cube image in comparison to the 2D FSE image in which the signal variation across the lesion appears more quantized.

In the unblinded review, a few instances demonstrated how the incorporation 3D T2-weighted images in breast MRI could affect the diagnostic information from T2-weighted images. In one case, a small (4 mm) presumed fibroadenoma based on three years of follow-up demonstrated contrast uptake on DCE images (Figure 5). The lesion is identifiable on both the respective 2D FSE and 3D-FSE-Cube images, however with notably different signal level with respect to the surrounding tissue. On 2D FSE, the lesion is hypointense while on the 3D-FSE-Cube images the lesion is hyperintense. T2-weighted hyperintensity in an enhancing lesion may be indicative that the lesion is benign, which aligns with the established designation of this lesion as a fibroadenoma. The reduced signal of the fibroadenoma in the 2D FSE image is due to the combination of the lesion signal with that of the surrounding tissue due to the thick slices. This is confirmed by the similar reduction in lesion signal intensity when two 3D-FSE-Cube slices are averaged (Figure 5d). In this case, the reduced signal of the small fibroadenoma due to the thick slices of 2D FSE may have erroneously indicated that the lesion was malignant while 3D-FSE-Cube may have improved specificity for the lesion.

In a second instance, the increased resolution of 3D-FSE-Cube facilitated the alignment of findings between the DCE and T2-weighted images. A benign papilloma demonstrated contrast uptake on DCE images (Figure 6). Benign papillomas can be particularly confounding in breast MRI as they demonstrate contrast uptake on DCE images that may be indicative of malignancy. However, there are morphologic and contrast characteristics that may help to identify a lesion as a papilloma. Papillomas often grow along a duct and have associated dilation of ducts that may demonstrate high T1 and T2-weighed signal (28,29). In the case of papillomas then, being able to reformat T2 images in a number of orientations could prove useful for deciphering the complex appearance of these lesions on MRI. In this case, there is high T2 signal associated with the lesion on both the corresponding 2D FSE and 3D-FSE-Cube images in the acquired axial plane. However, the elongated structure of the lesion is more clearly depicted in the DCE images reformatted into the sagittal plane (Figure 6d). The corresponding high T2-signal in the dilated duct is evident in the 3D-FSE-Cube sagittal reformats (Figure 6f) and can be clearly aligned with the morphology in the DCE reformats. However, because of the low through-plane resolution of 2D FSE, the respective sagittal images are severely blurred (Figure 6e). With 2D FSE, the clear depiction of lesion morphology in this papilloma is limited to the plane in which the data was acquired, but with 3D-FSE-Cube corroboration of morphology in the sagittal DCE image is possible.

## DISCUSSION

Although, T2-weighted imaging is a standard part of clinical breast MRI protocols, the contribution of T2-weighted images to differential diagnosis may be limited with conventional T2-weighted sequences. Three-dimensional T2-weighted sequences overcome these limitations and allow for the acquisition of high-resolution T2-weighted image

volumes in reasonable scan times. In this work we compared the 3D-FSE-Cube sequence with 2D FSE in 25 patients undergoing clinically indicated breast MRI. With 3D-FSE-Cube, the echo train length was increased by a factor of 4 in comparison to 2D FSE and acceleration with parallel imaging was available in 2 dimensions. As a result in 2/3 the scan time 3D-FSE-Cube provided a 50% reduction in voxel volume.

Analysis of contrast and depiction of morphology are important for the incorporation of 3D T2-weighted imaging into breast MRI because of the intricacies of these sequences. The contrast of 3D T2-weighted sequences like 3D-FSE-Cube reflects the combination of stimulated and spin echoes and therefore is dependent on the refocusing flip angle schedule. Similarly, assessment of depiction of lesion morphology is necessary due to the possible blurring as a result of the extended echo train (14). Our results show that both sequences demonstrated comparable contrast between lesions and fibroglandular tissue while 3D-FSE-Cube improved the depiction of lesion morphology in lesions with high T2 signal. The potential diagnostic contribution of the incorporation of 3D-FSE-Cube into routine breast MRI was demonstrated in 2 cases through better depiction of contrast in small lesions and improved alignment between DCE and T2-weighted findings.

One of the limitations of this study was the use of a single ROI to measure signal intensity, particularly in fibroglandular tissue. The distribution of fibroglandular tissue varies greatly from person to person while the T2 signal intensity of fibroglandular tissue also varies within an individual. While lesion ROIs were chosen based on the DCE images and effort was made to measure fibroglandular tissue signal in homogeneous regions, inevitably the signal measurements in both lesion and background contained some areas of heterogeneous signal. The average percent error (STD/Mean) was comparable both for lesion signal measurements and for fibroglandular tissue signal measurements for the two techniques (2D FSE fibroglandular tissue, 2D FSE lesion, 3D-FSE-Cube fibroglandular tissue, 3D-FSE-Cube lesion) demonstrating equivalent signal variability between the ROIs chosen with each technique.

For this study we chose to measure signal ratio between lesions and fibroglandular tissue because lesion T2 signal intensity relative to surrounding tissue can be utilized in differential diagnosis. T2-weighted images at our institution are acquired with fat suppression, however, another alternative is to acquire T2 images without fat suppression and assess T2 lesion signal relative to fat (1). We expect that the comparable contrast between 2D FSE and 3D-FSE-Cube demonstrated for a range of structures in this study would also occur with respect to fat as the reported T1 and T2 of fat in the breast (30) fall within the range of T1 and T2 values accommodated by 3D-FSE-Cube (14).

Though the sample size (10 lesions) in the blinded review of depiction of lesion morphology was small, the results are encouraging as 3D-FSE-Cube was chosen to have equivalent or improved depiction of lesion morphology in comparison to 2D FSE by all observers for all 10 lesions. It is also important to note that the average size of the 10 lesions was 8 mm × 8 mm. Depiction of lesion morphology in small lesions is particularly relevant as it can be very difficult to characterize lesions of < 5 mm on breast MRI. A frequent occurrence in breast MRI is small enhancing foci that can be very difficult to characterize (31,32). T2-weighted information is often not even available for these findings as the thick slices of conventional T2-weighted acquisitions may completely obscure the enhancing foci, or at the least make a confident alignment of the findings between DCE and T2-weighted images challenging. For example, while no enhancing lymph nodes were identified in this study, they present a type of lesion in which 3D T2-weighted imaging may prove to be especially useful due to their small size, distinct morphology, high T2-signal, and contrast uptake and washout erroneously indicative of malignancy. The potential for 3D T2-weighted imaging to

facilitate differential diagnosis in small enhancing foci is also demonstrated in the small enhancing fibroadenoma noted in the unblinded review (Figure 5). The high T2 signal intensity in this 5 mm × 5 mm lesion is more accurately depicted with 3D-FSE-Cube as a result of the higher through-plane resolution available with the sequence.

In the unblinded review, instances were noted that indicated the potential diagnostic contribution of 3D T2-weighted imaging in breast MRI. Improved through-plane resolution resulted in a more accurate depiction of lesion signal intensity in a small lesion surrounded by fat and the utility of being able to reformat the T2 data in any orientation allowed for lesion morphology to be analyzed in planes other than the acquisition plane. However, the fact that only 2 instances were noted for all 25 cases underscores that a much larger number of cases must be included in future analysis to confirm true diagnostic impact. One difference in image quality noted by both the blinded and unblinded reviewers was the consistency of fat suppression. Fat suppression was more consistent both across the breasts and from patient to patient with 2D FSE in comparison to 3D-FSE-Cube in which signal drop out was also evident in some cases at fat-water interfaces (Figure 3). Recently developed versions of 3D-FSE-Cube incorporate other fat suppression methods including IDEAL (33) and should be explored for future applications of 3D-FSE-Cube in the breast. While specific absorption rate (SAR) can be problematic for RARE imaging due to the repeated application of refocusing pulses with large flip angles, the variable refocusing flip angle schedules utilized in 3D T2-weighted images generally reduce RF power deposition despite the increased number of echoes acquired. SAR was never a limiting factor for the acquisition of 3D-FSE-Cube in this study.

In conclusion, we have demonstrated that 3D-FSE-Cube has comparable contrast to 2D FSE for a range of structures within the breast and that 3D-FSE-Cube improves the depiction of lesion morphology in lesions with high T2-signal. In addition, the means by which 3D T2-weighted imaging may contribute to differential diagnosis are demonstrated through examples of improved depiction of T2 lesion signal as well as improved alignment between DCE and T2-weighted findings with 3D-FSE-Cube. While a much larger study is needed to confirm diagnostic impact, these initial results demonstrate that the intricacies of 3D T2-weighted acquisitions do not undermine the potential for these techniques to expand the diagnostic information available in breast MRI.

## Acknowledgments

Grant Support: NIH 5T32CA09695, R01EB009055, R21EB012591, GE Healthcare

The authors would like to thank Dr. Emily McWalter for assistance with statistical analysis.

## References

1. Kuhl CK, Klaschik S, Mielcarek P, Gieseke J, Wardelmann E, Schild HH. Do T2-weighted pulse sequences help with the differential diagnosis of enhancing lesions in dynamic breast MRI? J Magn Reson Imaging. 1999; 9(2):187–196. [PubMed: 10077012]
2. Baltzer PA, Dietzel M, Kaiser WA. Nonmass lesions in magnetic resonance imaging of the breast: additional T2-weighted images improve diagnostic accuracy. J Comput Assist Tomogr. 2011; 35(3): 361–366. [PubMed: 21586932]
3. Ballesio L, Savelli S, Angeletti M, et al. Breast MRI:Are T2 IR sequences useful in the evaluation of breast lesions? Eur J Radiol. 2009; 71(1):96–101. [PubMed: 18479866]
4. Yuen S, Uematsu T, Kasami M, et al. Breast carcinomas with strong high-signal intensity on T2-weighted MR images: pathological characteristics and differential diagnosis. J Magn Reson Imaging. 2007; 25(3):502–510. [PubMed: 17326093]

5. Malich A, Fischer DR, Wurdinger S, et al. Potential MRI interpretation model: differentiation of benign from malignant breast masses. AJR Am J Roentgenol. 2005; 185(4):964–970. [PubMed: 16177416]
6. Liberman L, Morris EA, Lee MJ, et al. Breast lesions detected on MR imaging: features and positive predictive value. AJR Am J Roentgenol. 2002; 179(1):171–178. [PubMed: 12076929]
7. Lehman CD, Isaacs C, Schnall MD, et al. Cancer yield of mammography, MR, and US in high-risk women: prospective multi-institution breast cancer screening study. Radiology. 2007; 244(2):381–388. [PubMed: 17641362]
8. Mann RM, Kuhl CK, Kinkel K, Boetes C. Breast MRI: guidelines from the European Society of Breast Imaging. Eur Radiol. 2008; 18(7):1307–1318. [PubMed: 18389253]
9. Melki PS, Mulkern RV. Magnetization transfer effects in multislice RARE sequences. Magn Reson Med. 1992; 24(1):189–195. [PubMed: 1556927]
10. Hennig J, Nauerth A, Friedburg H. RARE imaging: a fast imaging method for clinical MR. Magn Reson Med. 1986; 3(6):823–833. [PubMed: 3821461]
11. Mugler JP 3rd, Bao S, Mulkern RV, et al. Optimized single-slab three-dimensional spin-echo MR imaging of the brain. Radiology. 2000; 216(3):891–899. [PubMed: 10966728]
12. Lichy MP, Wietek BM, Mugler JP 3rd, et al. Magnetic resonance imaging of the body trunk using a single-slab, 3-dimensional, T2-weighted turbo-spin-echo sequence with high sampling efficiency (SPACE) for high spatial resolution imaging: initial clinical experiences. Invest Radiol. 2005; 40(12):754–760. [PubMed: 16304477]
13. Hennig J, Weigel M, Scheffler K. Multiecho sequences with variable refocusing flip angles: optimization of signal behavior using smooth transitions between pseudo steady states (TRAPS). Magn Reson Med. 2003; 49(3):527–535. [PubMed: 12594756]
14. Busse RF, Hariharan H, Vu A, Brittain JH. Fast spin echo sequences with very long echo trains: design of variable refocusing flip angle schedules and generation of clinical T2 contrast. Magn Reson Med. 2006; 55(5):1030–1037. [PubMed: 16598719]
15. Alsop DC. The sensitivity of low flip angle RARE imaging. Magn Reson Med. 1997; 37(2):176–184. [PubMed: 9001140]
16. Stevens KJ, Busse RF, Han E, et al. Ankle: isotropic MR imaging with 3D-FSE-cube--initial experience in healthy volunteers. Radiology. 2008; 249(3):1026–1033. [PubMed: 19011194]
17. Shahid KR, Spinner RJ, Skinner JA, et al. Evaluation of intraneural ganglion cysts using three-dimensional fast spin echo-cube. J Magn Reson Imaging. 2010; 32(3):714–718. [PubMed: 20815072]
18. Kijowski R, Davis KW, Blankenbaker DG, Woods MA, Del Rio AM, De Smet AA. Evaluation of the menisci of the knee joint using three-dimensional isotropic resolution fast spin-echo imaging: diagnostic performance in 250 patients with surgical correlation. Skeletal Radiol. 2012; 41(2): 169–178. [PubMed: 21399933]
19. Agrawal G, Riherd JM, Busse RF, Hinshaw JL, Sadowski EA. Evaluation of uterine anomalies: 3D FRFSE cube versus standard 2D FRFSE. AJR Am J Roentgenol. 2009; 193(6):W558–562. [PubMed: 19933631]
20. Subhas N, Kao A, Freire M, Polster JM, Obuchowski NA, Winalski CS. MRI of the knee ligaments and menisci: comparison of isotropic-resolution 3D and conventional 2D fast spin-echo sequences at 3 T. AJR Am J Roentgenol. 2011; 197(2):442–450. [PubMed: 21785092]
21. Stevens KJ, Wallace CG, Chen W, Rosenberg JK, Gold GE. Imaging of the wrist at 1. 5 Tesla using isotropic three-dimensional fast spin echo cube. J Magn Reson Imaging. 2011; 33(4):908–915. [PubMed: 21448957]
22. Reeder SB, Pineda AR, Wen Z, et al. Iterative decomposition of water and fat with echo asymmetry and least-squares estimation (IDEAL): application with fast spin-echo imaging. Magn Reson Med. 2005; 54(3):636–644. [PubMed: 16092103]
23. Pineda AR, Reeder SB, Wen Z, Pelc NJ. Cramer-Rao bounds for three-point decomposition of water and fat. Magn Reson Med. 2005; 54(3):625–635. [PubMed: 16092102]
24. Reeder SB, McKenzie CA, Pineda AR, et al. Water-fat separation with IDEAL gradient-echo imaging. J Magn Reson Imaging. 2007; 25(3):644–652. [PubMed: 17326087]

25. Gold GE, Reeder SB, Yu H, et al. Articular cartilage of the knee: rapid three-dimensional MR imaging at 3. 0 T with IDEAL balanced steady-state free precession--initial experience. Radiology. 2006; 240(2):546–551. [PubMed: 16801369]

26. Brau AC, Beatty PJ, Skare S, Bammer R. Comparison of reconstruction accuracy and efficiency among autocalibrating data-driven parallel imaging methods. Magn Reson Med. 2008; 59(2):382–395. [PubMed: 18228603]

27. Beatty, PJ.; Brau, ACS.; Chang, S., et al. A method for autocalibrating 2-D accelerated volumetric parallel imaging with clinically practical reconstruction times. 15th Annual Meeting of ISMRM; Berlin, Germany. 2007. p. 1749

28. Bhattarai N, Kanemaki Y, Kurihara Y, Nakajima Y, Fukuda M, Maeda I. Intraductal papilloma: features on MR ductography using a microscopic coil. AJR Am J Roentgenol. 2006; 186(1):44–47. [PubMed: 16357375]

29. Kurz KD, Roy S, Saleh A, Diallo-Danebrock R, Skaane P. MRI features of intraductal papilloma of the breast: sheep in wolf's clothing? Acta Radiol. 2011; 52(3):264–272. [PubMed: 21498361]

30. Rakow-Penner R, Daniel B, Yu H, Sawyer-Glover A, Glover GH. Relaxation times of breast tissue at 1. 5T and 3T measured using IDEAL. J Magn Reson Imaging. 2006; 23(1):87–91. [PubMed: 16315211]

31. Dietzel M, Baltzer PA, Vag T, et al. Differential diagnosis of breast lesions 5 mm or less: is there a role for magnetic resonance imaging? J Comput Assist Tomogr. 2010; 34(3):456–464. [PubMed: 20498554]

32. Van den Bosch MA, Ikeda DM, Daniel BL. Doessize matter? Likelihood of cancer in MRI-detected lesions less than 5 mm AJR. Am J Roentgenol. 2007; 188(6):W571. [PubMed: 17515352]

33. Madhuranthakam AJ, Yu H, Shimakawa A, et al. T(2)-weighted 3D fast spin echo imaging with water-fat separation in a single acquisition. J Magn Reson Imaging. 2010; 32(3):745–751. [PubMed: 20815077]

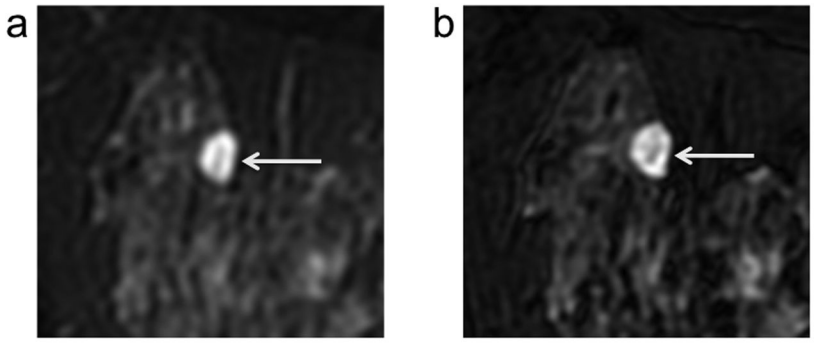


**Figure 1.**
Example case from blinded observer study of depiction of lesion morphology with 2D FSE (a) versus 3D-FSE-Cube (b). All three observers rated the clarity of depiction of lesion morphology in this cyst/hematoma (arrows) as better with 3D-FSE-Cube (b) versus 2D FSE (a) based on the increased gradation of signal levels evident within the lesion on 3D-FSE-Cube.

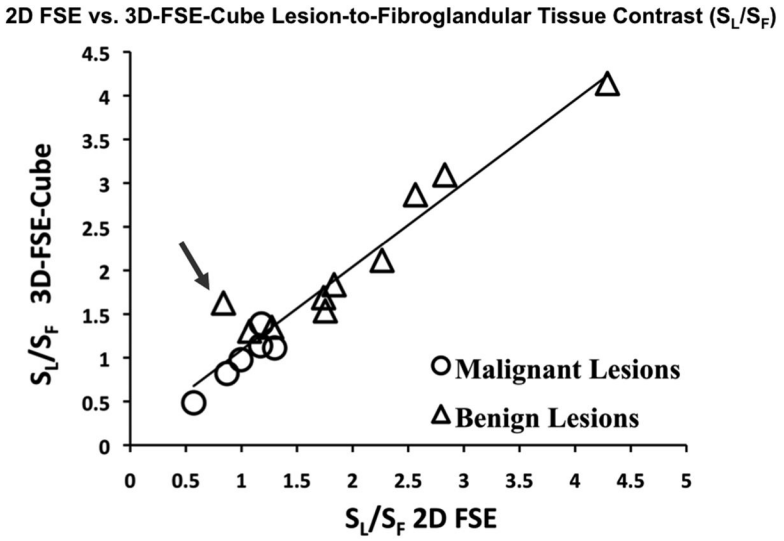


**Figure 2.**

Lesion-to-fibroglandular tissue signal ratio ($S_L/S_F$) is highly correlated between 2D FSE and 3D-FSE-Cube ($R^2 = 0.93$). The data point indicated by the arrow was measured in a very small fibroadenoma (images shown in Figure 5) in which partial voluming may have diminished the signal level in the lesion on 2D FSE, demonstrating a case in which the increased resolution available with 3D-FSE-Cube allows for a more accurate depiction of lesion signal intensity.

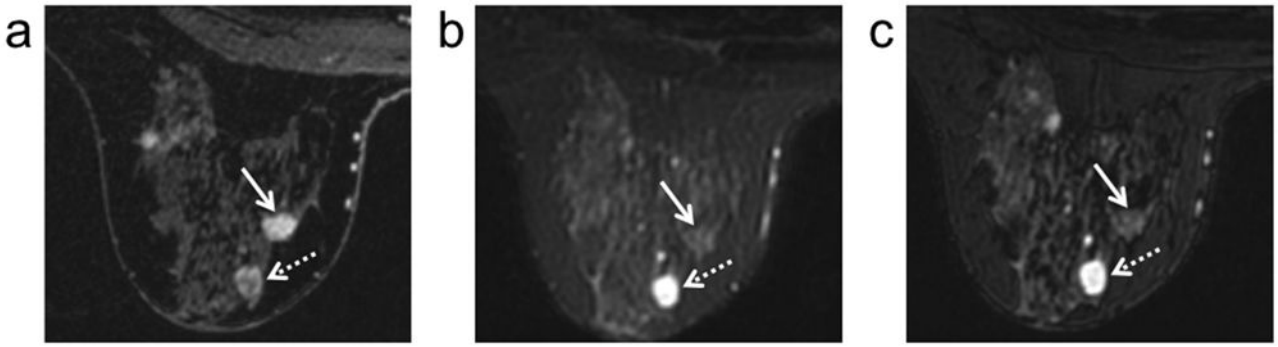


**Figure 3.**
DCE (100 seconds post injection) (a), 2D FSE (b), and 3D-FSE-Cube (c) images in a patient with invasive ductal carcinoma (solid arrows) and an enhancing fibroadenoma (dotted arrows) demonstrate the comparable contrast between 2D FSE and 3D-FSE-Cube in both enhancing benign and malignant lesions.

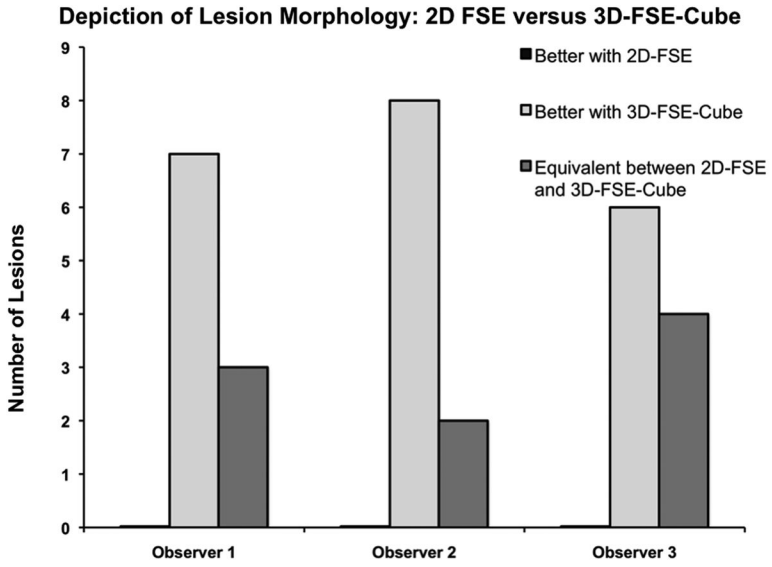


**Figure 4.**
In the blinded observer study, depiction of lesion morphology with 3D-FSE-Cube was chosen to be better or equivalent to that of 2D FSE for all cases.

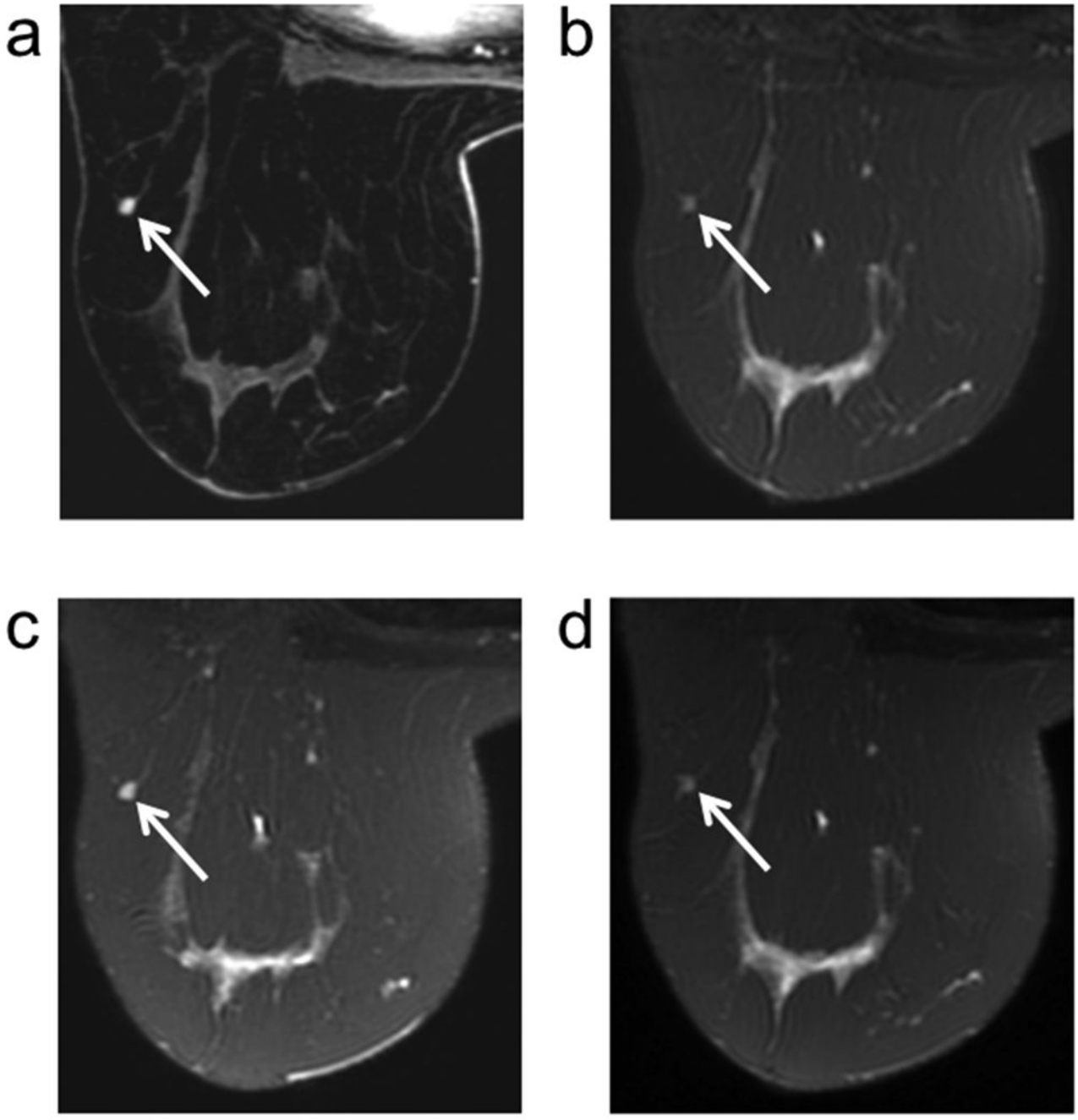


**Figure 5.**
A small presumed fibroadenoma (arrows) based on 3 years of follow-up demonstrates contrast uptake on the DCE (100 seconds post injection) image (a). With 2D FSE (b), the lesion signal is hypointense, a possible indication of malignancy. With 3D-FSE-Cube (c) the lesion signal is hyperintense and thus aligns with the expected T2 contrast behavior of a fibroadenoma. The difference in contrast is the result of the difference in slice thickness of the two techniques as opposed to an inherent contrast difference between 3D-FSE-Cube and 2D FSE as demonstrated by the same reduction in signal intensity when two 3D-FSE-Cube slices are averaged together (d).

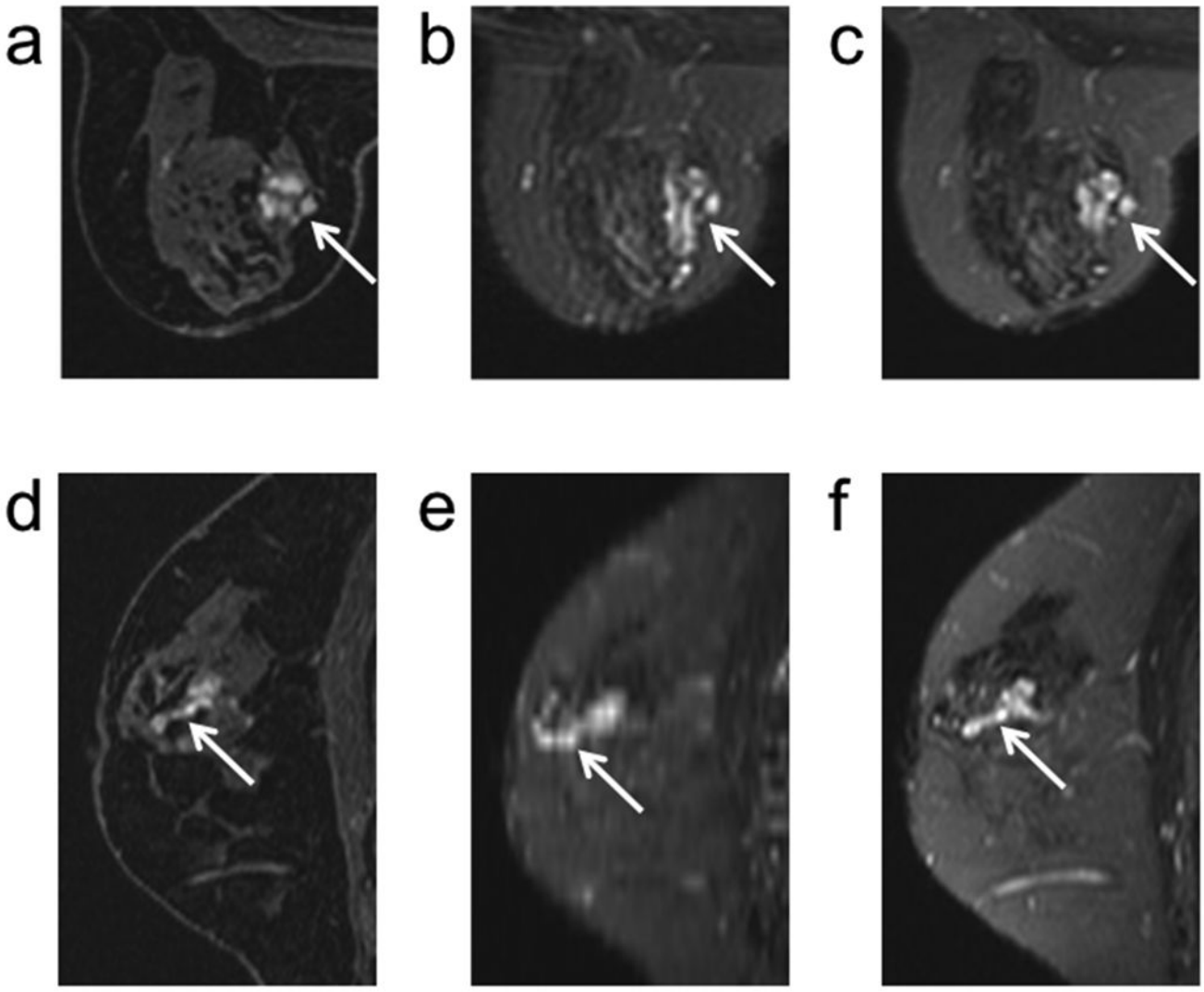


**Figure 6.**

A benign papilloma (arrows) demonstrates contrast uptake on an axial DCE (100 seconds post injection) image (a). The high signal intensity of the dilated ducts associated with a papilloma on T2-weighted images is evident on both the corresponding axial 2D FSE (b) and 3D-FSE-Cube (C) images. The elongated structure of the papilloma along a duct is depicted on a sagittal reformat of the DCE image (d). Comparable depiction of the dilated duct in a sagittal reformat is not available with 2D FSE (e) but the higher through-plane resolution of 3D-FSE-Cube (f) allows for clear depiction of the dilated duct and thus facilitates alignment of the DCE and corresponding T2 morphology in the sagittal reformats.